Prochlorococcus rely on microbial interactions rather than on chlorotic resting stages to survive long-term nutrient starvation

Dalit Roth-Rosenberg[a*], Dikla Aharonovich[a*], Tal Luzzatto-Knaan[a*], Angela Vogts[b], Luca Zoccarato[c], Falk Eigemann[b], Noam Nago[a], Hans-Peter Grossart[c,d], Maren Voss[b] and Daniel Sher #[a]

[a] Department of Marine Biology, Leon H. Charney School of Marine Sciences, University of Haifa, 199 Aba Khoushy Ave. Mount Carmel, Haifa 3498838, Israel.

[b] Leibniz-Institute for Baltic Sea Research, Seestrasse 15, D-18119 Warnemuende, Germany.

[c] Department of Experimental Limnology, Leibniz-Institute of Freshwater Ecology and Inland Fisheries, Alte Fischerhuette 2, D-16775 Stechlin, Germany.

[d] Potsdam University, Institute of Biochemistry and Biology, Maulbeeralle 2, D-14469 Potsdam, Germany.

Running title: Interactions and starvation in *Prochlorococcus*

Corresponding author: dsher@univ.haifa.ac.il

*Dalit Roth-Rosenberg, Dikla Aharonovich, Tal Luzzatto-Knaan contributed equally to this study.

Word count for the abstract: 166

Word count for the text: 4,420

Abstract

Many microorganisms produce resting cells with very low metabolic activity that allow them to survive phases of prolonged nutrient or energy stress. In cyanobacteria and some eukaryotic phytoplankton, the production of resting stages is accompanied by a loss of photosynthetic pigments, a process termed chlorosis. Here, we show that a chlorosis-like process occurs under multiple stress conditions in axenic laboratory cultures of *Prochlorococcus*, the dominant phytoplankton linage in large regions of the oligotrophic ocean and a global key player in ocean biogeochemical cycles. In *Prochlorococcus* strain MIT9313, chlorotic cells show reduced metabolic activity, measured as C and N uptake by NanoSIMS. However, unlike many other cyanobacteria, chlorotic *Prochlorococcus* cells are not viable and do not re-grow under axenic conditions when transferred to new media. Nevertheless, co-cultures with a heterotrophic bacterium, *Alteromonas macleodii* HOT1A3, allowed *Prochlorococcus* to survive nutrient starvation for months. We propose that reliance on co-occurring heterotrophic bacteria, rather than the ability to survive extended starvation as resting cells, underlies the ecological success of *Prochlorococcus*.

Importance

The ability of microorganisms to withstand long periods of nutrient starvation is key to their survival and success under highly fluctuating conditions as is common in nature. Therefore, one would expect this trait to be prevalent among organisms in the nutrient-poor open ocean. Here, we show that this is not the case for *Prochlorococcus*, a globally abundant and

45 ecologically impactful marine cyanobacterium. Instead, *Prochlorococcus* rely on co-occurring
46 heterotrophic bacteria to survive extended phases of nutrient and light starvation. Our results
47 highlight the power of microbial interactions to drive major biogeochemical cycles in the ocean
48 and elsewhere with consequences at the global scale.
49

50 **Introduction**

51 Not all microbial cells living in natural environments are equally active. In aquatic
52 environments, up to 90% of the cells do not exhibit measurable metabolic activity ("vitality"),
53 based on dyes (e.g. that assess electron transport) or on uptake assays with labeled substrates
54 (1). Several possible and non-exclusive explanations have been proposed for this heterogeneity.
55 First, "observed differences in activity between cells in natural populations may represent
56 inherent differences in activity between genetically-different organisms, e.g. due to variations
57 in maximum growth rate or the ability to utilize the specific substrate tested. Second, cells
58 might be at different physiological states, e.g. exponentially growing, starved or dying, and thus
59 exhibiting different levels of metabolic activity (2, 3). Third, cells show stochastic fluctuations in
60 their activity, due to noise in gene expression or regulatory networks (4). Finally, some
61 organisms respond to environmental stress by producing resting stages or spores. Such cells
62 often exhibit very low (or undetectable) metabolic activity, yet are viable, namely able to return
63 to an active state and reproduce when environmental conditions return to favorable (5). The
64 presence of such resting stages, together with a fluctuating activity at the single-cell level and
65 the genetic variability found within natural populations, are suggested to promote the survival
66 of the population as a whole (2, 6).

67 Understanding the factors affecting the metabolic activity (vitality) of phytoplankton is
68 of special interest. These microbial primary producers perform about one-half of the
69 photosynthesis on Earth, providing energy through carbon fixation at the base of the aquatic
70 ecosystem (7). As phytoplankton grow, they take up elements such as nitrogen (N) and
71 phosphorus (P) from the environment, potentially leading to low nutrient concentrations that
72 may constrain the growth of both the phytoplankton themselves and co-occurring organisms
73 (8, 9). Phytoplankton viability, including their ability to survive under conditions of nutrient
74 stress, has been extensively studied, especially for organisms that produce massive blooms that
75 emerge and decline rapidly (reviewed by (10-12)). For example, some bloom-forming
76 cyanobacteria such as *Aphanizomenon* species produce morphologically-distinct spores that
77 show very little photosynthetic activity, yet remain viable in the sediment for long periods of
78 time, providing the inoculum for the next growth season (13). In laboratory cultures of
79 *Synechococcus elegantus* PCC 7942 and *Synechocystis* PCC 6803, two unicellular freshwater
80 cyanobacteria, nitrogen starvation results in a programmed process where cells enter a resting
81 stage, enabling them to survive prolonged periods of stress (14, 15). As part of this process,
82 cells degrade their photosynthetic apparatus in a controlled manner, resulting in a loss of
83 chlorophyll autofluorescence and culture bleaching (a process termed chlorosis). However, the
84 observation that chlorotic cells are viable resting stages is not universal. Chlorotic cultures of
85 *Microcystis aeruginosa* PCC 7806 were shown to contain a small population of non-chlorotic
86 cells with high chlorophyll autofluorescence (described throughout this study as "high-fl"). Only
87 these high-fl cells were suggested to revive after the re-addition of a nitrogen source, while the
88 low-fl cells are presumably dead (16). Chlorotic cells were also observed in eukaryotic

89 phytoplankton, however it is not yet clear to what extent such cells remain viable, as it may
90 depend on the specific organism and stress conditions (11, 17, 18).

91 *Prochlorococcus* is a pico-cyanobacterium that is extremely abundant in the oligotrophic
92 oceans, performing an estimated ~8.5% of global ocean photosynthesis (19). The carbon fixed
93 by *Prochlorococcus*, which are estimated to produce up to 75% of the daily photosynthetic
94 carbon in the surface layer of the Pacific subtropical gyre (20), can then be utilized by co-
95 occurring heterotrophic bacteria. *Prochlorococcus* cells in the oceans exhibit extremely high
96 genetic diversity (21), and some of this diversity has been linked with their ability to grow under
97 conditions of extreme nutrient limitation (e.g. (22, 23)). It has therefore been suggested that
98 this genetic diversity enables *Prochlorococcus* as a group to thrive across a wide variety of
99 oceanic conditions (24). While the physiological and transcriptional responses of multiple
100 *Prochlorococcus* lineages to short-term nutrient starvation have been extensively studied (e.g.
101 (22, 25-29)), little is known about their ability to survive more than a few days under such
102 conditions. A study on the response of *Prochlorococcus* strains to a different type of stress,
103 extended darkness (i.e. C starvation), has shown that these organisms can survive light
104 starvation only for a limited time (30). In these experiments, low-fl cell populations reminiscent
105 of chlorotic cells in other cyanobacteria appeared after the light-starved cultures were re-
106 exposed to light (30). Therefore, phenotypic evidence exists that *Prochlorococcus* can undergo a
107 chlorosis-like process, yet whether these chlorotic cells are active, and whether they are resting
108 stages that can resume growth when conditions are favorable, is currently unknown. Our
109 experiments were therefore designed to answer the following questions: i) Do *Prochlorococcus*
110 respond to long-term nutrient starvation by producing chlorotic cells? ii) If so, are such cells

111 metabolically active (vital) and are they able to reproduce and grow when stress conditions end
112 (viable)? To address these questions, we used fluorescence-activated cell sorting (FACS) to
113 obtain distinct chlorotic sub-populations from axenic and unialgal laboratory cultures of
114 *Prochlorococcus* which were pre-incubated with isotopically-labelled tracers for photosynthesis
115 ($H^{13}CO_3$) and nutrient uptake ($^{15}NH_4^+$) and we visualized their activity using Nanoscale
116 Secondary Ion Mass Spectrometry (NanoSIMS). This method enabled us to measure
117 photosynthesis and N uptake at a single cell resolution by quantifying the change in isotopic
118 ratios (31, 32). Our results show that while *Prochlorococcus* do undergo a chlorosis-like process,
119 with some of the chlorotic cells still photosynthesizing and taking up NH_4^+, the chlorotic cells
120 are unable to re-grow and thus do not represent resting stages. Instead, co-culture with
121 heterotrophic bacteria enables *Prochlorococcus* to survive long-term stress even without
122 producing resting stages.
123

124 **Results and discussion**

125 **Emergence of chlorotic sub-populations in *Prochlorococcus* cultures**

126 As *Prochlorococcus* batch cultures reach stationary stage and start declining, the green color of
127 the cultures disappears, and sub-populations of cells emerge with lower chlorophyll
128 autofluorescence that can be identified by flow cytometry (Fig. 1A, B). This phenomenon is
129 observed in strains from all major cultured ecotypes, as well as in a marine *Synechococcus*,
130 strain WH8102 (Fig. 1C). In the high-light adapted strain *Prochlorococcus* MIT9312, lower
131 chlorophyll populations emerged in batch cultures that reached stationary stage due to both N
132 and P limitation, although the timing of sub-population emergence and the forward light

133 scatter and chlorophyll autofluorescence (analyzed by flow cytometry) were different under the
134 two nutrient stresses (Fig. S1A, B, (33)). Cells with lower chlorophyll autofluorescence also
135 appeared in populations of another strain, the low-light adapted MIT9313, when these cultures
136 were inhibited in a co-culture with high cell densities of the heterotrophic bacterium
137 *Alteromonas* HOT1A3 (Fig. S1C, D (34)). Thus, the emergence of populations of cells with lower
138 chlorophyll autofluorescence under a variety of stress conditions is a pervasive phenomenon
139 across marine pico-cyanobacteria. We focused our experiments aiming to better characterize
140 this phenomenon on *Prochlorococcus* strain MIT9313, as the response to stress in this strain
141 has been extensively studied (e.g. (22, 26, 27, 34-36)). Additionally, in this strain, three clearly
142 separate sub-populations can be observed when cultured in Pro99 media, facilitating the
143 sorting and subsequent NanoSIMS analyses (Fig. 1B, referred to throughout the study as high-,
144 mid- and low-fl populations).

145 **Assessing the metabolic activity of sorted chlorotic sub-populations**

146 We next asked whether the high, mid- and low-fl populations differ in their vitality, measured
147 here as their photosynthesis and nutrient uptake rates (incorporation of $H^{13}CO_3^-$ and $^{15}NH_4^+$,
148 respectively). The uptake ratio of labeled versus unlabeled nutrients were then used to
149 calculate the metabolic activity of the sorted cells (Table 1). As shown in Fig. 2 and Table 1, the
150 mean uptake of both $H^{13}CO_3^-$ and $^{15}NH_4^+$ was highest in the high-fl population, followed by the
151 mid and low-fl populations, with the latter population indistinguishable from the control, i.e.
152 glutaraldehyde-killed cells. We have repeated the entire workflow in an independent

153 experiment, and the results are very similar (Fig. S2A, B, Table 1). These results are reminiscent

154 of observations in several eukaryotic phytoplankton (18).

Strain and growth stage	Sub-population	Illumination	V^C (fg cell^{-1} day^{-1})	V^N (fg cell^{-1} day^{-1})
MIT9313, exponential growth*	High	Constant light 27 µE	12.92 ± 11.93	2.74 ± 2.43
MIT9313, old cultures **	High	Constant light 27 µE	2.67-2.77 ± 2.89-3.57	0.62-0.69 ± 0.54-0.63
	Mid		0.75-0.79 ± 1.73-1.78	0.25-0.32 ± 0.42-0.35
	Low		0.09-0.14 ± 0.52-0.67	0.08-0.14 ± 0.15-0.12
MIT9313, old culture***	High	Photo-period 12:12 L/D, 27 µE	1.01 ± 2.67	0.32 ± 0.33
	Mid		0.48 ± 2.47	0.20 ± 0.20
	Low		0.13 ± 0.31	0.14 ± 0.11

155 **Table 1**

156 Calculated mean C and N uptake rates from the experiments performed with *Prochlorococcus*

157 MIT9313. The means and standard deviation were calculated from the uptake rates values of

158 single cells in each experiment.

159 *The results for MIT9313 exponential growth refer to the experiment presented in Fig. S3.

160 **The results for old MIT9313 cultures under constant light refer to the two experiments

161 presented in Fig. 2 and Fig. S2A, B.

162 *** The results for Old MIT9313 cultures under L/D refer to the experiment presented in Fig.

163 S2C-F. The experiment was sampled after a longer period due to slower growth under a light-

164 dark cycle compared with constant light (Fig. S2C).

165 The mean uptake rates for glutaraldehyde killed cells (control) were 0.06±0.15 fg cell-1 day-1
166 for C and 0.18±0.02 fg cell-1 day-1 for N, and most likely depict the absorption of the label by
167 non-specific binding or diffusion.
168
169 Within each of the populations, cell-cell heterogeneity was observed in both ^{13}C and ^{15}N
170 uptake (Fig. 2, Fig. S2A,B). Within all of the populations (including the high-fl), some cells were
171 inactive, and this could not be explained by the limited purity of the FACS-sorting procedure
172 (Table S1, supplementary text). The coefficients of variation in C and N uptake rates were
173 within the range shown for other organisms, or higher (Table S2 (32, 37)). Similar levels of
174 heterogeneity (primarily in N uptake) were also seen in cells grown under a 12:12 light-dark
175 cycle, where the *Prochlorococcus* cell-cycle follows a diel rhythm, suggesting that this
176 heterogeneity is not due to different stages of the cell cycle or the diel cycle (Table S2, Fig. S2C-
177 F). Cell-cell heterogeneity was also observed in cells from an exponentially-growing, nutrient-
178 replete culture (Fig. S3, Table S2), suggesting that this heterogeneity is not exclusively limited to
179 ageing or stressed cells. This is in accordance with studies assessing the vitality of
180 *Prochlorococcus* cells using various dyes, which consistently show that a significant fraction of
181 the cells in laboratory cultures are inactive or potentially dead (38, 39).

182 In addition to differing in their chlorophyll autofluorescence and metabolic activity, the
183 high-, mid- and low-fl cell populations also differ by their forward and side light scatter
184 properties, which are related to cell size and (in larger cells) morphological complexity (Fig. S4A,
185 B). In agreement with these observations, cells sorted from the high-fl population and observed

186 by SEM (Scanning Electron Microscopy) were 20-30% larger than those from the mid- and low-fl
187 populations (Fig. S4C-E).

188

189 **Evaluating the viability of sub-populations**

190 We next asked whether the low-fl cells are viable resting stages. We tested this indirectly by
191 determining the ability of *Prochlorococcus* MIT9313 cells, cultured in Pro99 media, to grow
192 upon transfer to new growth media at different times during exponential growth and upon
193 culture decline. As shown in Fig. 3A, only cells from cultures where the high-fl cells were
194 dominant could grow when transferred to new growth media. No growth was observed upon
195 transfer of cells from stationary or declining cultures where no high-fl cells were observed.
196 Intriguingly, the presence of high-fl cells was not enough to ensure culture growth (e.g. day 34
197 in Fig. 3A). This is consistent with a previous study showing that cells belonging to a different
198 *Prochlorococcus* strain, MED4, that were incubated for three days in the dark, were unable to
199 resume growth after return to light despite showing no clear difference in the chlorophyll
200 autofluorescence (30). The probability of growth after transfer did not depend on the number
201 of transferred cells (40), with as many as 2.5×10^7 cells/ml failing to grow after transfer during
202 culture decline (cells at ~1/10 of this density grew after being transferred during exponential
203 stage). Thus, non-chlorotic cells (defined as being within the range of chlorophyll
204 autofluorescence exhibited by exponentially-growing cells) are not necessarily viable.

205 One problem with performing experiments in Pro99, which is commonly used to culture
206 *Prochlorococcus*, is that the conditions causing cells to reach stationary stage are not always

207 clear (e.g. (41). We therefore repeated these experiments under conditions where entry into
208 stationary phase is induced by N or P starvation (Fig. 3B, Fig. S5, (42)). When entry into
209 stationary stage was induced by N or P starvation, chlorotic cells appeared much faster, and the
210 cultures became non-viable much earlier – essentially immediately after the cessation of
211 exponential growth. Similar results were obtained with a different strain of *Prochlorococcus*,
212 MIT9312 (Fig. S5A, B). However, a marine *Synechococcus* (strain WH8102) behaved differently,
213 surviving N starvation much longer and being able to re-grow in nutrient replete media long
214 after the culture started declining, and when essentially all cells were chlorotic (Fig. S5D). This is
215 reminiscent of the ability of (presumably axenic) cultures of two freshwater cyanobacteria,
216 *Synechococcus* PCC 7942 and *Synechocystis* PCC 6803, to revive after extended N starvation (14,
217 15).

218

219 The inability of axenic *Prochlorococcus* strains to survive long-term nutrient starvation
220 was surprising, and we therefore hypothesized that their survival would be enhanced by
221 interactions with co-occurring heterotrophic bacteria. Indeed, when co-cultured with a
222 heterotrophic bacterium, *Alteromonas* HOT1A3 (34, 43), *Prochlorococcus* strains representing
223 all major cultured ecotypes were able to re-grow after 60 days of N and P stress, whereas all
224 axenic strains failed to do so (Fig. 4, Fig. S6A, B). Interestingly, strain MIT9313, which was
225 initially inhibited by this *Alteromonas* strain (Fig. 4A, (34, 44)), was also able to survive long-
226 term starvation in co-culture, suggesting that fundamentally different interactions occur during
227 exponential growth compared to long-term, presumably nutrient-limited growth. These results

228 are consistent with the ability of heterotrophic bacteria to extend the survival time of different
229 *Prochlorococcus* strains under conditions of constant darkness (albeit for only several days,
230 (30)) and with the ability of different heterotrophic bacteria to support the long-term viability
231 of batch cultures of *Synechococcus* WH7803 (45). We observed similar results when
232 *Prochlorococcus* cultures were transferred from nutrient-replete media into sterile sea water
233 with no added nutrients (Fig. S6C, D). This suggests that the ability of the heterotrophs to
234 support *Prochlorococcu*s survival is due to nutrient remineralization rather than to the
235 detoxification of potential waste products, although a potential role for de-toxification cannot
236 be ruled out (45).

237

238 **Stress survival in pico-cyanobacteria: why is *Prochlorococcus* different?**

239 In this study, we demonstrate that phenotypic heterogeneity between clonal *Prochlorococcus*
240 cells occurs at multiple "scales". In exponentially growing axenic laboratory cultures of two
241 strains, MIT9313 and MED4, C and N uptake rates differ significantly between individual cells
242 (summarized in Table S2). This variation is independent of genetic variability. Additionally, as
243 axenic cultures become stressed, a larger phenotypic change occurs as cells lose their
244 chlorophyll auto-fluorescence and become chlorotic. Under these experimental conditions,
245 most cells are inactive (primarily in the low-fl population, as measured in strain MIT9313),
246 although we cannot rule out that even low-fl cells still retain a residual level of activity not
247 detectable by the nanoSIMS. Nevertheless, some cells from the chlorotic populations retain at
248 least part of their photosynthetic capacity, and indeed can fix carbon and take up NH_4. Yet, in

249 our experiments, they do not re-grow when condition become more favorable. In
250 *Synechococcus elegantus* PCC 7942, chlorotic cultures retain approximately 0.01% of their
251 photosynthetic activity, as well as a residual level of protein translation, although it remains
252 unclear whether this is a process shared by all cells in the culture or whether this activity is only
253 due to a small subset of more active cells (14). The clear difference between the ability of
254 axenic *Synechococcus elegantus* PCC 7942 and *Synechocystis* PCC6803 to survive long-term N
255 starvation, and the inability of axenic *Prochlorococcus* cultures to do so, suggests an inherent
256 difference in the physiology and genomic functional capacity between these unicellular
257 cyanobacteria.

258 Entry into chlorosis in *Synechocystis* is a regulated process that involves the organized
259 degradation of the phycobilisomes in parallel with an increase in the storage products glycogen
260 and polyhydroxybutyrate (PHB) (15). The photosynthesis apparatus of *Prochlorococcus* is
261 different from that of other cyanobacteria, using unique chlorophyll a2/b2 binding proteins
262 rather than phycobilisomes (46). Indeed, *Prochlorococcus* lack orthologs of the nblA gene
263 required for phycobilisome degradation during chlorosis (15). Additionally, while
264 *Prochlorococcus* likely use glycogen as a C storage pool (47), they lack the phaA-C and phaE
265 genes required for PHB biosynthesis and which are induced in *Synechocystis* PCC 6803 under
266 chlorosis (although these genes are not required for revival from chlorosis (15)). Taken
267 together, these differences suggest that *Prochlorococcus* lack the genetic toolkit employed by
268 *Synechocystis* PCC6803 and *Synechococcus elegantus* PCC7942 to enter into a resting stage.
269 Thus, chlorotic cells in *Prochlorococcus* are not resting stages. However, we note that
270 *Synechococcus* WH8102 also lacks the gene nblA gene, yet can survive N starvation much longer

271 in axenic culture than the tested *Prochlorococcus* strains can (Fig. S5D). This suggests that
272 additional molecular mechanisms besides nblA-mediated degradation of the phycobilisomes
273 are important for long-term survival of nutrient starvation in *Synecococcus* WH8102.

274 If *Prochlorococcus* are indeed incapable of producing resting stages in response to nutrient or
275 light starvation, what are the evolutionary drivers of this phenotype, and what are the
276 consequences for the dynamics of *Prochlorococcus* populations in the ocean? While the open
277 oligotrophic ocean is often considered a relatively stable environment, nutrient concentrations
278 do fluctuate (8), and phytoplankton (including *Prochlorococcus*) inhabiting these waters show
279 multiple signs of nutrient stress (48). Many of the microbes that live in such environments
280 comprising a large fraction of the surface ocean have small, highly streamlined genomes (49)
281 and this has been suggested to be an adaptation to low nutrient concentrations (24, 49, 50) .
282 Therefore, it is possible that the lack of resting stages is a result of this genome streamlining -
283 the genomes of *Synechococcus elegantus* PCC7942 and *Synechocystis* PCC6803 are ~3.2mbp
284 and ~4 mbp with their plasmids, respectively, compared to ~1.4-2.5 mbp for *Prochlorococcus*
285 strains.

286

287 **Surviving nutrient stress "with a little help from my friends".**

288 The ability of *Prochlorococcus* to thrive under conditions of extreme nutrient limitation is often
289 explained by their small cell size (increasing their biomass-specific diffusion), their generally low
290 nutrient requirements, and their specific metabolic strategies to minimize the per-cell
291 elemental quotas (51-53). However, these mechanisms appear not to work in axenic laboratory

292 cultures, and thus we propose that interactions with co-occurring microorganisms enable
293 *Prochlorococcus* to survive when nutrient-saving mechanisms are not sufficient, as suggested
294 for its close relative *Synechococcus* (45). This may take the form of recycling of inorganic
295 nutrients by the heterotrophic bacteria, as well as possibly by the production of organic
296 compounds that contain elements such as N or P. Indeed, *Prochlorococcus* can compete with
297 heterotrophic bacteria for amino acids (54). Importantly, the utilization of organic compounds
298 (mixotrophy) may provide *Prochlorococcus* also with carbon, sulfur or energy sources, and may
299 potentially help them survive also light starvation (e.g. (30, 55-59)).

300 Regardless of the specific forms of dissolved organic matter being utilized by the cells, and on
301 the exact mechanism enabling the cells to survive long-term nutrient starvation in co-culture,
302 the lack of any observed mechanism for the production of resting stages by *Prochlorococcus*
303 may be considered another manifestation of the "Black Queen Hypothesis". This hypothesis
304 states that microorganisms "outsource" essential survival mechanisms such as detoxification of
305 reactive oxygen species to the surrounding microbial community (60). These forms of microbial
306 interactions likely affect the distribution and activity of *Prochlorococcus* on a global scale. The
307 increased survival of *Prochlorococcus* under harsh conditions, supported by its associated
308 heterotrophic bacteria, may enable it to remain active at the single cell level even during long
309 periods of unfavorable conditions (61, 62). Thus, the tight interactions between
310 *Prochlorococcus* and its bacterial "supporters" likely affects photosynthesis and carbon cycling
311 at the base of the aquatic foodweb, with potentially profound implications for overall oceanic
312 productivity and carbon cycling.

313

314 **Material and Methods**

315 ***Prochlorococcus* growth and Stable Isotope Incubations**

316 Axenic *Prochlorococcus* strains were grown in Pro99 media under constant cold while light
317 (27 µE) at 22 °C. Axenicity of the strains was tested routinely, as well as before all major
318 experiments, using test media (ProMM, (40)). Additionally, no evidence for contaminating
319 heteroteophic cells was observed in flow cytometry, scanning electron microscopy or when
320 axenic *Prochlorococcus* cultures were used as negative controls for 16S amplicon sequencing.
321 Bulk chlorophyll fluorescence (FL) (ex440; em680) was measured almost daily using a
322 Fluorescence Spectrophotometer (Cary Eclipse, Varian). In parallel, samples for flow cytometry
323 were taken for cell numbers. When three distinct sub-populations appeared in the flow
324 cytometry, the cultures were labeled with 1mM Sodium bicarbonate-^{13}C and 1mM Ammonium-
325 ^{15}N chloride (Sigma-Aldrich, USA) for 18-24 hours. The optimal incubation time based on
326 preliminary isotope labeling experiments with *Prochlorococcus* MED4, showing that uptake is
327 identified already after 3 hours and is linear until 24 hours under our growth conditions (Fig.
328 S7). Incubations were stopped by fixing 2 ml of the culture with 2X EM grade glutaraldehyde
329 (2.5% final concentration, Sigma) and subsequently storing at 4 °C until the sorting analysis.
330 Non-labeled cells that were killed before labeling (by adding 2.5% glutaraldehyde) were used as
331 a negative control.

332

333 **Cell Sorting and Filtration**

334 Sorting of sub-population was carried out using a BD FACSAria III sorter (BD Biosciences) at the Life
335 Sciences and Engineering Infrastructure Center, Technion, Israel. Each sample was sorted for 3 sub-
336 populations: Non-chlorotic (High-fl), Semi chlorotic (Mid-fl) and Chlorotic (Low-fl) (Fig. 2A). The sorting
337 gates for each sub-population were determined from the population observed in forward scatter (FSC, a
338 proxy for cell size) and auto-fluorescence (PerCP, chlorophyll auto-fluorescence). After sorting, the
339 sorted sup-population were gently filtered on 13 mm diameter polycarbonate filters (GTTP, 0.2 µM pore
340 size, Millipore, MA), washed twice with sterile sea water and air-dried. The filters were cut into two
341 parts. One half was stored at 4°C until nanoSIMS analyses and the other half is for Scanning Electron
342 Microscopy.
343

344 **Nanoscale secondary ion mass spectrometry (nanoSIMS) and data analysis**

345 The samples were coated with a layer of ca. 30 nm gold with a Cressington 108 auto sputter
346 coater (Watford, United Kingdom). Random spots were employed for NanoSIMS analyses. SIMS
347 imaging was performed using a NanoSIMS 50L instrument (Cameca, Paris, France) at the
348 Leibniz-Institute for Baltic Sea Research Warnemünde (IOW). A $^{133}Cs^{+}$ primary ion beam was
349 used to erode and ionize atoms of the sample. Images of secondary electrons, $^{12}C^{-}$, $^{13}C^{-}$, $^{12}C^{14}N^{-}$
350 and $^{12}C^{15}N^{-}$ were recorded simultaneously using mass detectors equipped with electron
351 multipliers (Hamamatsu). The mass resolving power was adjusted to be sufficient to suppress
352 interferences at all masses allowing, e.g. the separation of $^{13}C^{-}$ from interfering ions such as
353 $^{12}C^{1}H^{-}$. Prior to the analysis, sample areas of 50×50 µm were sputtered for 2 min with 600 pA to
354 erode the gold, clean the surface and reach the steady state of secondary ion formation. The
355 primary ion beam current during the analysis was 1 pA; the scanning parameters were 512×512

356 pixels for areas of 30x30 to 48x48 µm, with a dwell time of 250 µs per pixel. 60 planes were
357 analysed.
358

359 **Analyses of NanoSIMS measurements**

360 All NanoSIMS measurements were analysed with the Matlab based program look@nanosims
361 (63). Briefly, the 60 measured planes were checked for inconsistencies and all usable planes
362 accumulated, regions of interest (ROI's) (i.e. *Prochlorococcus* cells and filter regions without
363 organic material for background measurements) defined based on $^{12}C^{14}N$ mass pictures, and
364 $^{13}C/^{12}C$ as well as $^{12}C^{15}N/^{12}C^{14}N$ ratios calculated from the ion signals for each region of interest.

365

366 **Uptake rate calculation**

367 Uptake rate was estimated using the following equation, based on that of (64), as follows:

$$V = \frac{(\%P_t^* - \%P_0^*)}{(\%D_i^* - \%D_0^*)}\frac{Q}{t}$$

368 Where $\%P^*_t$ is the concentration (atom %) of the heavy isotope in the particulate matter at the
369 end of the incubation, $\%D^*_i$ is the concentration of the dissolved tracer added to the incubation
370 (and assumed not to change over the short incubation time), and $\%P^*_0$ and $\%D^*_0$ are the
371 natural heavy isotope concentrations in the particulate and dissolved matter, respectively. We
372 estimated *Q*, the cell quota (in fg cell^{-1}) of C or N, based on measurements of the biomass of
373 MED4 and MIT9313 (66 fg cell^{-1}and 158 fg cell^{-1}, respectively, (65)) and assuming that C
374 comprises 50% and N comprises 7.5% of the cell biomass. For heavy isotopes concentration in

375 the particulate and dissolved phases before incubation we used the natural values for isotopic
376 ratios of ^{13}C and ^{15}N (1.12% and 0.37% respectively). For the experiment shown in Fig. S7, we
377 measured the NH_4^+ concentration in the media and added the ^{15}N tracer to 50% final
378 concentration. Since all other experiments were performed in declining cultures we assumed
379 that the NH_4^+ was depleted from the media, and thus $\%D^*_t$ was defined as 90%, based on
380 previous measurements of NH_4^+ concentrations in old cultures. We used a value of 50% for the
381 initial percentage of ^{13}C, based on dissolved inorganic carbon (DIC) measurements (42). For the
382 terminal concentrations of ^{15}N and ^{13}C in the particulate phase ($\%P^*_t$) we used the values of
383 $^{13}C/^{12}C$ and $^{15}N/^{14}N$ that were obtained from the NanoSims analysis of the cells. $^{13}C/^{12}C$ and
384 $^{15}N/^{14}N$ below the natural values resulted with negative uptake values, and were treated as
385 zero uptake.

386 Mean and standard deviation of C and N uptake rates were calculated from the uptake rate
387 values of individual cells (Table 1). The uptake rate values were not corrected for negative
388 control (killed cells), which are presented for comparison in table 1. Since $^{13}C/^{12}C$ and $^{15}N/^{14}N$
389 values of individual cells were not normally distributed, for significance analysis we used non-
390 parametric tests (Mann-Whitney and Kruskal-Wallis tests) performed using the Real Statistics
391 Resource Pack software (Release 5.4 www.real-statistics.com).

392

393 **Scanning Electron Microscopy**

394 Immediately after filtration, filters dehydrated in an ethanol series of 30%, 50%, 70%, 80%, 90% and
395 100% (vol/vol) ethanol (dilutions were in deionized water) for 10 min each. Samples were then dried,

396 mounted on stubs with carbon tape and coated with 5 nm with gold. Cells were obtained on a ZEISS
397 SigmaTM SEM, by using a SE2 detector (2–2.5 kV, WD = 8 mm).

398

399 **Acknowledgements**

400 We thank Annett Grüttmüller for NanoSIMS routine operation. This study was supported by
401 grant RGP0020/2016 from the Human Frontiers Science Program (to MV, HPG and DS) and by
402 grant number 1635070/2016532 from the NSF-BSF program in Oceanography (NSFOCE-BSF, to
403 DS). The NanoSIMS at the Leibnitz-Institute for Baltic Sea research in Warnemuende (IOW) was
404 funded by the German Federal Ministry of Education and Research (BMBF), grant identifier
405 03F0626A.

406

407 **Author contributions**

408 DRR, DA, TLK, AV, MV and DS designed experiments, DRR, DA, TLK, LZ, NN and DS performed
409 experiments and field analyses, DRR, DA, TLK, AV, and FE performed NanoSIMS analyses, DRR,
410 DA, TLK, AV, LZ, FE, NN, HPG, MV and DS analyzed results, DRR, DA, TLK and DS wrote
411 manuscript with contributions from all authors.

412

413 **Competing interests**

414 The authors declare no competing interests

415

416 **Materials and Correspondence**

Please send requests for materials or other correspondence to Daniel Sher, dsher@univ.haifa.ac.il

References:

1. Del Giorgio PA, Gasol JM. Physiological Structure and Single-Cell Activity in Marine Bacterioplankton. In: Kirchman DL, editor. Microbial Ecology of the Oceans2008.
2. Bergkessel M, Basta DW, Newman DK. The physiology of growth arrest: uniting molecular and environmental microbiology. Nat Rev Microbiol. 2016;14:549.
3. Jørgensen BB, Lever MA, Rogers KL, Lloyd KG, Overmann J, Schink B, et al. Life under extreme energy limitation: a synthesis of laboratory- and field-based investigations. FEMS Microbiology Reviews. 2015;39(5):688-728.
4. Engl C. Noise in bacterial gene expression. Biochemical Society Transactions. 2018:BST20180500.
5. Harms A, Maisonneuve E, Gerdes K. Mechanisms of bacterial persistence during stress and antibiotic exposure. Science. 2016;354(6318):aaf4268.
6. Lennon JT, Jones SE. Microbial seed banks: the ecological and evolutionary implications of dormancy. Nat Rev Microbiol. 2011;9(2):119-30.
7. Field CB, Behrenfeld MJ, Randerson JT, Falkowski P. Primary Production of the Biosphere: Integrating Terrestrial and Oceanic Components. Science. 1998;281(5374):237-40.
8. Moore CM, Mills MM, Arrigo KR, Berman-Frank I, Bopp L, Boyd PW, et al. Processes and patterns of oceanic nutrient limitation. Nat Geosci. 2013;6(9):701-10.
9. Bratbak G, Thingstad TF. Phytoplankton-Bacteria Interactions - an Apparent Paradox - Analysis of a Model System with Both Competition and Commensalism. Mar Ecol-Prog Ser. 1985;25(1):23-30.
10. Kirchman DL. Oceanography - Phytoplankton death in the sea. Nature. 1999;398(6725):293-4.
11. Franklin DJ, Brussaard CPD, Berges JA. What is the role and nature of programmed cell death in phytoplankton ecology? Eur J Phycol. 2006;41(1):1-14.
12. Bidle KD. The Molecular Ecophysiology of Programmed Cell Death in Marine Phytoplankton. Ann Rev Mar Sci. 2015;7(1):341-75.
13. Sukenik A, Maldener I, Delhaye T, Viner-Mozzini Y, Sela D, Bormans M. Carbon assimilation and accumulation of cyanophycin during the development of dormant cells (akinetes) in the cyanobacterium Aphanizomenon ovalisporum. Frontiers in Microbiology. 2015;6(1067).
14. Sauer J, Schreiber U, Schmid R, Völker U, Forchhammer K. Nitrogen Starvation-Induced Chlorosis in Synechococcus PCC 7942. Low-Level Photosynthesis As a Mechanism of Long-Term Survival. Plant Physiology. 2001;126(1):233-43.
15. Klotz A, Georg J, Bučinská L, Watanabe S, Reimann V, Januszewski W, et al. Awakening of a Dormant Cyanobacterium from Nitrogen Chlorosis Reveals a Genetically Determined Program. Current Biology. 2016;26(21):2862-72.
16. de Abreu Meireles D, Schripsema J, Vetö Arnholdt AC, Dagnino D. Persistence of Only a Minute Viable Population in Chlorotic Microcystis aeruginosa PCC 7806 Cultures Obtained by Nutrient Limitation. PLOS ONE. 2015;10(7):e0133075.
17. Behrenfeld MJ, Falkowski PG. Photosynthetic rates derived from satellite-based chlorophyll concentration. Limnol Oceanogr. 1997;42(1):1-20.

18. Veldhuis MJW, Kraay GW, Timmermans KR. Cell death in phytoplankton: correlation between changes in membrane permeability, photosynthetic activity, pigmentation and growth. Eur J Phycol. 2001;36(2):167-77.
19. Flombaum P, Gallegos JL, Gordillo RA, Rincón J, Zabala LL, Jiao N, et al. Present and future global distributions of the marine Cyanobacteria Prochlorococcus and Synechococcus. Proceedings of the National Academy of Sciences. 2013;110(24):9824-9.
20. Ribalet F, Swalwell J, Clayton S, Jiménez V, Sudek S, Lin Y, et al. Light-driven synchrony of Prochlorococcus growth and mortality in the subtropical Pacific gyre. Proceedings of the National Academy of Sciences. 2015;112(26):8008-12.
21. Kashtan N, Roggensack SE, Rodrigue S, Thompson JW, Biller SJ, Coe A, et al. Single-Cell Genomics Reveals Hundreds of Coexisting Subpopulations in Wild Prochlorococcus. Science. 2014;344(6182):416-20.
22. Martiny AC, Coleman ML, Chisholm SW. Phosphate acquisition genes in Prochlorococcus ecotypes: evidence for genome-wide adaptation. Proc Natl Acad Sci U S A. 2006;103(33):12552-7.
23. Berube PM, Rasmussen A, Braakman R, Stepanauskas R, Chisholm SW. Emergence of trait variability through the lens of nitrogen assimilation in Prochlorococcus. eLife. 2019;8:e41043.
24. Biller SJ, Berube PM, Lindell D, Chisholm SW. Prochlorococcus: the structure and function of collective diversity. Nat Rev Microbiol. 2014;13:13.
25. Steglich C, Behrenfeld M, Koblizek M, Claustre H, Penno S, Prasil O, et al. Nitrogen deprivation strongly affects Photosystem II but not phycoerythrin level in the divinyl-chlorophyll b-containing cyanobacterium Prochlorococcus marinus. Biochimica et Biophysica Acta (BBA) - Bioenergetics. 2001;1503(3):341-9.
26. Tolonen AC, Aach J, Lindell D, Johnson ZI, Rector T, Steen R, et al. Global gene expression of Prochlorococcus ecotypes in response to changes in nitrogen availability. Mol Syst Biol. 2006;2:53.
27. Thompson AW, Huang K, Saito MA, Chisholm SW. Transcriptome response of high- and low-light-adapted Prochlorococcus strains to changing iron availability. Isme J. 2011;5(10):1580-94.
28. Krumhardt KM, Callnan K, Roache-Johnson K, Swett T, Robinson D, Reistetter EN, et al. Effects of phosphorus starvation versus limitation on the marine cyanobacterium Prochlorococcus MED4 I: uptake physiology. Environ Microbiol. 2013;15(7):2114-28.
29. Domínguez-Martín MA, Gómez-Baena G, Díez J, López-Grueso MJ, Beynon RJ, García-Fernández JM. Quantitative Proteomics Shows Extensive Remodeling Induced by Nitrogen Limitation in Prochlorococcus marinus SS120. mSystems. 2017;2(3):e00008-17.
30. Coe A, Ghizzoni J, LeGault K, Biller S, Roggensack SE, Chisholm SW. Survival of Prochlorococcus in extended darkness. Limnol Oceanogr. 2016;61(4):1375-88.
31. Gao D, Huang X, Tao Y. A critical review of NanoSIMS in analysis of microbial metabolic activities at single-cell level. Critical Reviews in Biotechnology. 2016;36(5):884-90.
32. Berthelot H, Duhamel S, L'Helguen S, Maguer J-F, Wang S, Cetinić I, et al. NanoSIMS single cell analyses reveal the contrasting nitrogen sources for small phytoplankton. The ISME Journal. 2018.
33. Grossowicz M, Marques GM, van Voorn GAK. A dynamic energy budget (DEB) model to describe population dynamics of the marine cyanobacterium Prochlorococcus marinus. Ecol Model. 2017;359:320-32.
34. Aharonovich D, Sher D. Transcriptional response of Prochlorococcus to co-culture with a marine Alteromonas: differences between strains and the involvement of putative infochemicals. ISME J. 2016;10(12):2892-906.
35. Domínguez-Martín MA, López-Lozano A, Clavería-Gimeno R, Velázquez-Campoy A, Seidel G, Burkovski A, et al. Differential NtcA Responsiveness to 2-Oxoglutarate Underlies the Diversity of C/N Balance Regulation in Prochlorococcus. Frontiers in Microbiology. 2018;8(2641).

36. Domínguez-Martín MA, López-Lozano A, Rangel-Zúñiga OA, Díez J, García-Fernández JM. Distinct features of C/N balance regulation in Prochlorococcus sp. strain MIT9313. FEMS microbiology letters. 2017;365(3).
37. Matantseva O, Skarlato S, Vogts A, Pozdnyakov I, Liskow I, Schubert H, et al. Superposition of Individual Activities: Urea-Mediated Suppression of Nitrate Uptake in the Dinoflagellate Prorocentrum minimum Revealed at the Population and Single-Cell Levels. Frontiers in Microbiology. 2016;7(1310).
38. Agusti S, Sanchez MC. Cell viability in natural phytoplankton communities quantified by a membrane permeability probe. Limnol Oceanogr. 2002;47(3):818-28.
39. Hughes C, Franklin DJ, Malin G. Iodomethane production by two important marine cyanobacteria: Prochlorococcus marinus (CCMP 2389) and Synechococcus sp. (CCMP 2370). Marine Chemistry. 2011;125(1–4):19-25.
40. Morris JJ, Kirkegaard R, Szul MJ, Johnson ZI, Zinser ER. Facilitation of robust growth of Prochlorococcus colonies and dilute liquid cultures by "helper" heterotrophic bacteria. Appl Environ Microbiol. 2008;74(14):4530-4.
41. Moore LR, Coe A, Zinser ER, Saito MA, Sullivan MB, Lindell D, et al. Culturing the marine cyanobacterium Prochlorococcus. Limnol Oceanog Methods. 2007;5:353-62.
42. Grossowicz M, Roth-Rosenberg D, Aharonovich D, Silverman J, Follows MJ, Sher D. Prochlorococcus in the lab and in silico: The importance of representing exudation. Limnol Oceanogr. 2017;62(2):818-35.
43. Fadeev E, De Pascale F, Vezzi A, Hübner S, Aharonovich D, Sher D. Why close a bacterial genome? The plasmid of Alteromonas macleodii HOT1A3 is a vector for inter-specific transfer of a flexible genomic island. Frontiers in Microbiology. 2016;7.
44. Sher D, Thompson JW, Kashtan N, Croal L, Chisholm SW. Response of Prochlorococcus ecotypes to co-culture with diverse marine bacteria. Isme J. 2011;5(7):1125-32.
45. Christie-Oleza JA, Sousoni D, Lloyd M, Armengaud J, Scanlan DJ. Nutrient recycling facilitates long-term stability of marine microbial phototroph–heterotroph interactions. Nature Microbiology. 2017;2:17100.
46. Ting CS, Rocap G, King J, Chisholm SW. Cyanobacterial photosynthesis in the oceans: the origins and significance of divergent light-harvesting strategies. Trends in Microbiology. 2002;10(3):134-42.
47. Lichtlé C, Thomas JC, Spilar A, Partensky F. Immunological and ultrastructural characterization of the photosynthetic complexes of the prochlorophyte Prochlorococcus (Oxychlorobacteria). Journal of Phycology. 1995;31(6):934-41.
48. Saito MA, McIlvin MR, Moran DM, Goepfert TJ, DiTullio GR, Post AF, et al. Multiple nutrient stresses at intersecting Pacific Ocean biomes detected by protein biomarkers. Science. 2014;345(6201):1173-7.
49. Yooseph S, Nealson KH, Rusch DB, McCrow JP, Dupont CL, Kim M, et al. Genomic and functional adaptation in surface ocean planktonic prokaryotes. Nature. 2010;468:60.
50. Giovannoni SJ. SAR11 Bacteria: The Most Abundant Plankton in the Oceans. Ann Rev Mar Sci. 2017;9(1):231-55.
51. Van Mooy BA, Rocap G, Fredricks HF, Evans CT, Devol AH. Sulfolipids dramatically decrease phosphorus demand by picocyanobacteria in oligotrophic marine environments. Proc Natl Acad Sci U S A. 2006;103(23):8607-12.
52. Gilbert JDJ, Fagan WF. Contrasting mechanisms of proteomic nitrogen thrift in Prochlorococcus. Mol Ecol. 2011;20(1):92-104.
53. Read RW, Berube PM, Biller SJ, Neveux I, Cubillos-Ruiz A, Chisholm SW, et al. Nitrogen cost minimization is promoted by structural changes in the transcriptome of N-deprived Prochlorococcus cells. The ISME journal. 2017;11(10):2267-78.

554 54. Zubkov MV, Tarran GA, Fuchs BM. Depth related amino acid uptake by Prochlorococcus
555 cyanobacteria in the Southern Atlantic tropical gyre. Fems Microbiol Ecol. 2004;50(3):153-61.
556 55. Muñoz-Marín MdC, Luque I, Zubkov MV, Hill PG, Diez J, García-Fernández JM. Prochlorococcus
557 can use the Pro1404 transporter to take up glucose at nanomolar concentrations in the Atlantic Ocean.
558 Proceedings of the National Academy of Sciences. 2013;110(21):8597-602.
559 56. Vila-Costa M, Simó R, Harada H, Gasol JM, Slezak D, Kiene RP. Dimethylsulfoniopropionate
560 Uptake by Marine Phytoplankton. Science. 2006;314(5799):652-4.
561 57. Becker JW, Hogle SL, Rosendo K, Chisholm SW. Co-culture and biogeography of Prochlorococcus
562 and SAR11. The ISME Journal. 2019.
563 58. Rocap G, Larimer FW, Lamerdin J, Malfatti S, Chain P, Ahlgren NA, et al. Genome divergence in
564 two Prochlorococcus ecotypes reflects oceanic niche differentiation. Nature. 2003;424(6952):1042-7.
565 59. Yelton AP, Acinas SG, Sunagawa S, Bork P, Pedrós-Alió C, Chisholm SW. Global genetic capacity
566 for mixotrophy in marine picocyanobacteria. The Isme Journal. 2016;10:2946.
567 60. Morris JJ, Lenski RE, Zinser ER. The Black Queen Hypothesis: Evolution of Dependencies through
568 Adaptive Gene Loss. mBio. 2012;3(2).
569 61. Ma L, Calfee BC, Morris JJ, Johnson ZI, Zinser ER. Degradation of hydrogen peroxide at the
570 ocean's surface: the influence of the microbial community on the realized thermal niche of
571 Prochlorococcus. The Isme Journal. 2017;12:473.
572 62. Hennon GMM, Morris JJ, Haley ST, Zinser ER, Durrant AR, Entwistle E, et al. The impact of
573 elevated CO2 on Prochlorococcus and microbial interactions with 'helper' bacterium Alteromonas. The
574 Isme Journal. 2017;12:520.
575 63. Polerecky L, Adam B, Milucka J, Musat N, Vagner T, Kuypers MM. Look@NanoSIMS--a tool for
576 the analysis of nanoSIMS data in environmental microbiology. Environ Microbiol. 2012;14(4):1009-23.
577 64. Legendre L, Gosselin M. Estimation of N or C uptake rates by phytoplankton using 15N or 13C:
578 revisiting the usual computation formulae. J Plankt Res. 1997;19(2):263-71.
579 65. Cermak N, Becker JW, Knudsen SM, Chisholm SW, Manalis SR, Polz MF. Direct single-cell
580 biomass estimates for marine bacteria via Archimedes' principle. The Isme Journal. 2016;11:825.

581

582

583 **FIG 1**

584 Emergence of chlorotic sub-populations in *Prochlorococcus* batch cultures as measured by flow
585 cytometry. (A) A representative growth curve of an axenic culture of MIT9313, grown in Pro99.
586 The arrows mark the days shown in panel B. (B) Flow cytometry scattergrams at the marked
587 time-points from the MIT9313 culture. The x-axis is Forward Scatter (FSC, a proxy for cell size)
588 and the y-axis is the chlorophyll autofluorescence of the cells (Per-CP). The emergence of
589 chlorotic sub-population observed from the late exponential phase (Day 18). (C) Chlorotic sub-
590 population observed in ageing batch cultures of *Prochlorococcus*, belonging to different
591 ecotypes: High-Light adapted MED4 (HLI), MIT9312 (HLII) and Low-Light adapted NATL2A (LLI)
592 and MIT9313 (LLIV). In all strains, the chlorotic G cells begin to emerge at late growth stage,
593 becoming dominant in declining cultures, while in the exponential phase only one population
594 can be observed. Additional growth curves for this strain and for others, including replicates
595 and standard deviations, as shown in Fig. 3 and 4 and in Fig. S1-3, and S5-6.

596

597 **FIG 2**

598 Metabolic activity of sorted sub-populations by NanoSIMS (A) Flow cytometry scatterplots
599 before and after sorting of three distinct sub-populations (high, mid and low-fl) of an aging
600 *Prochlorococcus* MIT9313 culture, detected by flow cytometry. The cultures were grown for 30
601 days in Pro99 and labeled with $H^{13}CO_3^-$ and $^{15}NH_4^+$ for 18h. (B) NanoSIMS images of $^{15}N/0^{12}C$
602 analysis of killed cells (negative control) and high, mid and low-fl cells after sorting. (C)
603 Scatterplot of $^{13}C/^{12}C$ and $^{15}N/^{14}N$ ratios obtained from NanoSIMS analysis of each sub-

604 population. (D, E) Boxplots of the $^{13}C/^{12}C$ and $^{15}N/^{14}N$ enrichment in each sub-population. Lines
605 represent the median, X represents the mean, box borders are 1st quartiles and whiskers
606 represent the full range.

607

608 **FIG 3**

609 Time-dependent changes in viability of cells transferred into fresh media at different life cycle
610 stages of a batch culture for MIT9313 in Pro99 (A-C) and when stationary stage is induced by N
611 starvation (D-F). (A, D) Growth curves of a MIT9313 culture, in Pro99 media commonly used for
612 *Prochlorococcus* culturing (A) and under conditions where stationary stage is induced by
613 nitrogen starvation (panel (D), 2:1 N/P ratio in the growth media, (42)). Colored circles indicate
614 the times point at which triplicate 1ml samples were transferred into 20 ml fresh media. (B, E)
615 Flow cytometry scatterplots of the culture shown in panels (A) and (D). Note that, under
616 conditions of N starvation, the cultures shift rapidly from being comprised primarily of high-fl
617 cells (day 19 in panel (E), early stationary phase) to mainly mid-fl cells, with essentially no high-
618 fl cells (day 21 in panel (E). (C, F) Growth curves of cells being transferred at different times to
619 new, nutrient-replete media (assessed via bulk culture fluorescence). In these plots, each line
620 shows a replicate culture. Cells could not re-grow when transferred after more than 31 days in
621 Pro99 and 17 days of nitrogen starvation. This suggests that, in this strain, high-fl cells are not
622 necessarily viable.

623

624 **FIG 4**

625 Co-culture with a heterotrophic bacterium, *Alteromonas* HOT1A3, enables multiple
626 *Prochlorococcus* strains to survive long-term N starvation. (A) 10^6 axenic *Prochlorococcus* cells
627 ml^{-1} from different strains were incubated alone (green line) or with the addition of 10^7
628 *Alteromonas* HOT1A3 cells ml^{-1} in low-N media (grey line). Bulk culture fluorescence was
629 recorded as a proxy for cell growth, and 1ml from each culture was transferred into 25ml fresh
630 Pro99 media after 60 days. Panel (B) The transferred cultures were recorded for additional 40
631 days. Error bars are standard deviation from triplicate cultures. The late growth of MIT9313 in
632 co-culture is the "delayed growth" phenotype described in (34, 44). (C) Flow cytometry
633 scattergrams of the cultures shown in panel A. Co-culture with *Alteromonas* increases the
634 number of *Prochlorococcus* cells seen by flow cytometry, suggesting a reduction in the
635 magnitude of mortality (cell lysis). A decrease in per-cell chlorophyll autofluorescence is still
636 seen, suggesting co-culture does not completely inhibit the process of chlorophyll degradation.

637

FIG 1

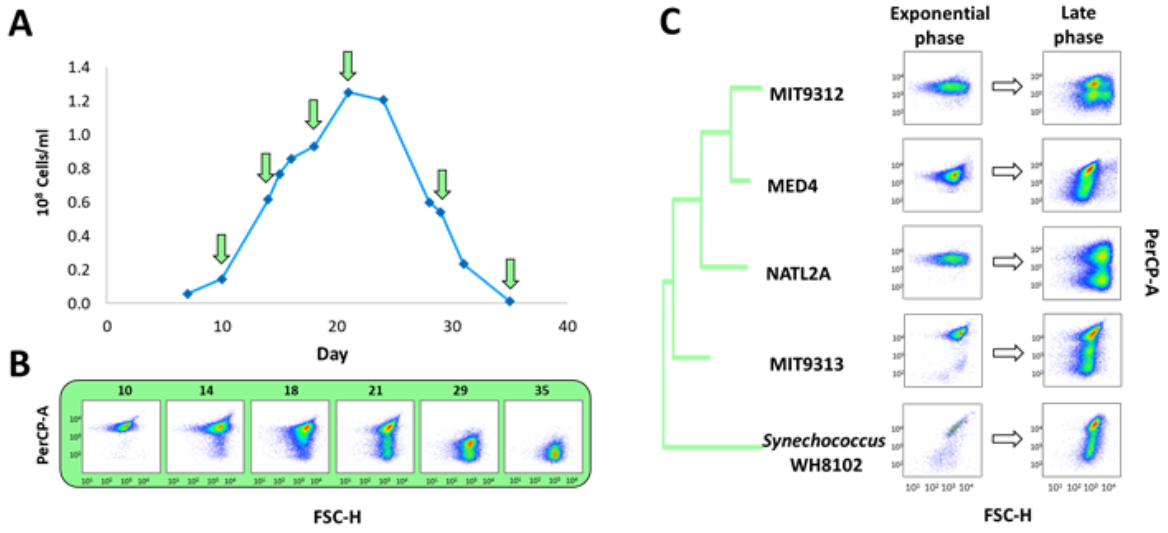
A
1.4
1.2
1.0
0.8
0.6
0.4
0.2
0.0
10^8 Cells/ml
0
10
20
30
40
Day
B
10
14
18
21
29
35
PerCP-A
FSC-H
C
Exponential phase
Late phase
MIT9312
MED4
NATL2A
MIT9313
Synechococcus WH8102
PerCP-A
FSC-H

FIG 2

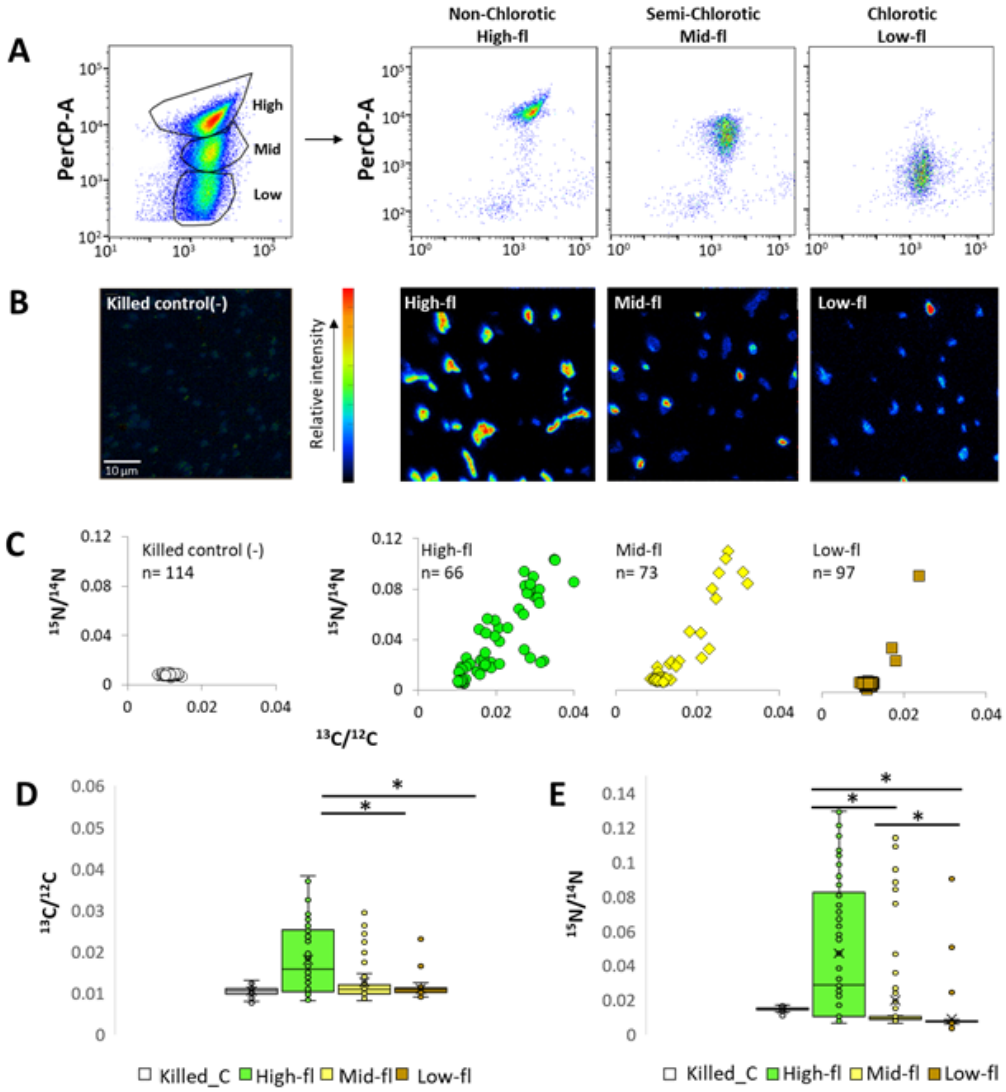
A
Non-Chlorotic
High-fl
Semi-Chlorotic
Mid-fl
Chlorotic
Low-fl
PerCP-A
High
Mid
Low
B
Killed control(-)
Relative intensity
10 µm
High-fl
Mid-fl
Low-fl
C
Killed control (-)
n= 114
High-fl
n= 66
Mid-fl
n= 73
Low-fl
n= 97
15N/14N
13C/12C
D
13C/12C
Killed_C
High-fl
Mid-fl
Low-fl
E
15N/14N
Killed_C
High-fl
Mid-fl
Low-fl

FIG 3

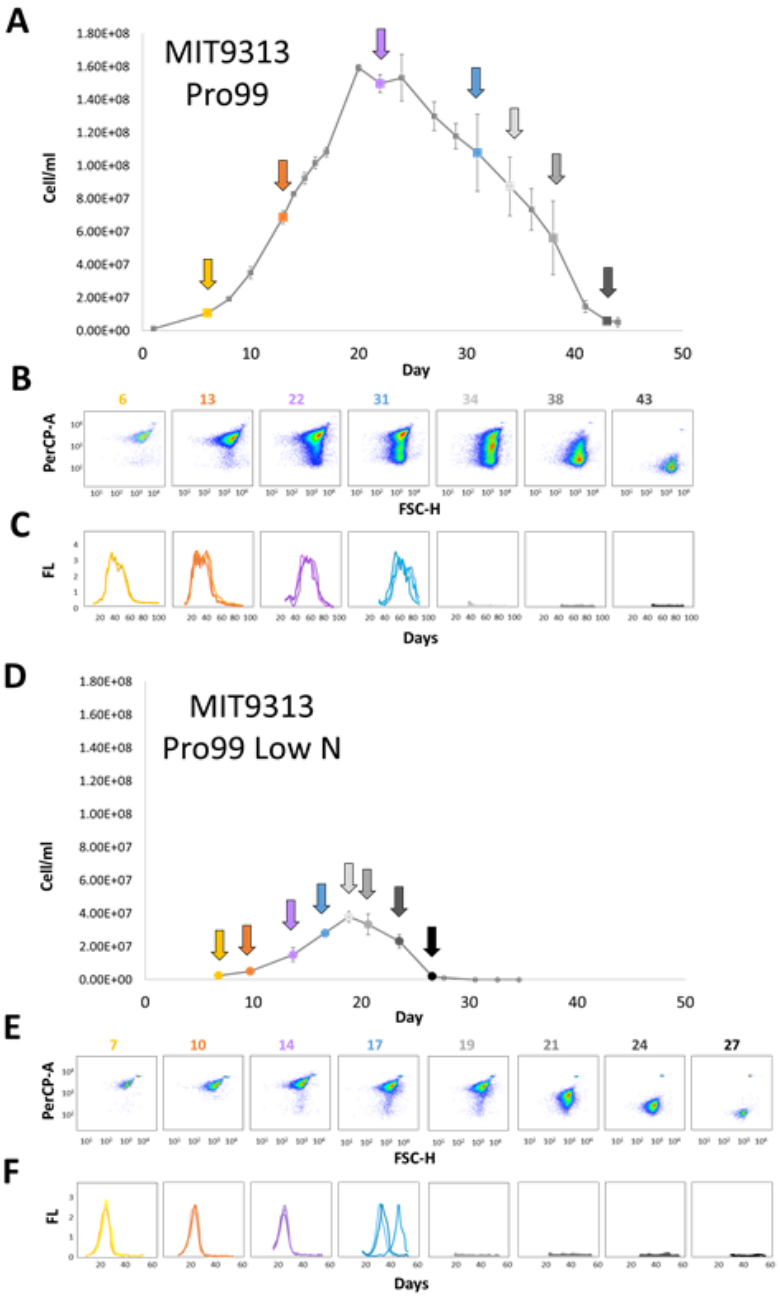
A
MIT9313
Pro99
Cell/ml
Day
B
6
13
22
31
34
38
43
PerCP-A
FSC-H
C
FL
Days
D
MIT9313
Pro99 Low N
Cell/ml
Day
E
7
10
14
17
19
21
24
27
PerCP-A
FSC-H
F
FL
Days

FIG 4

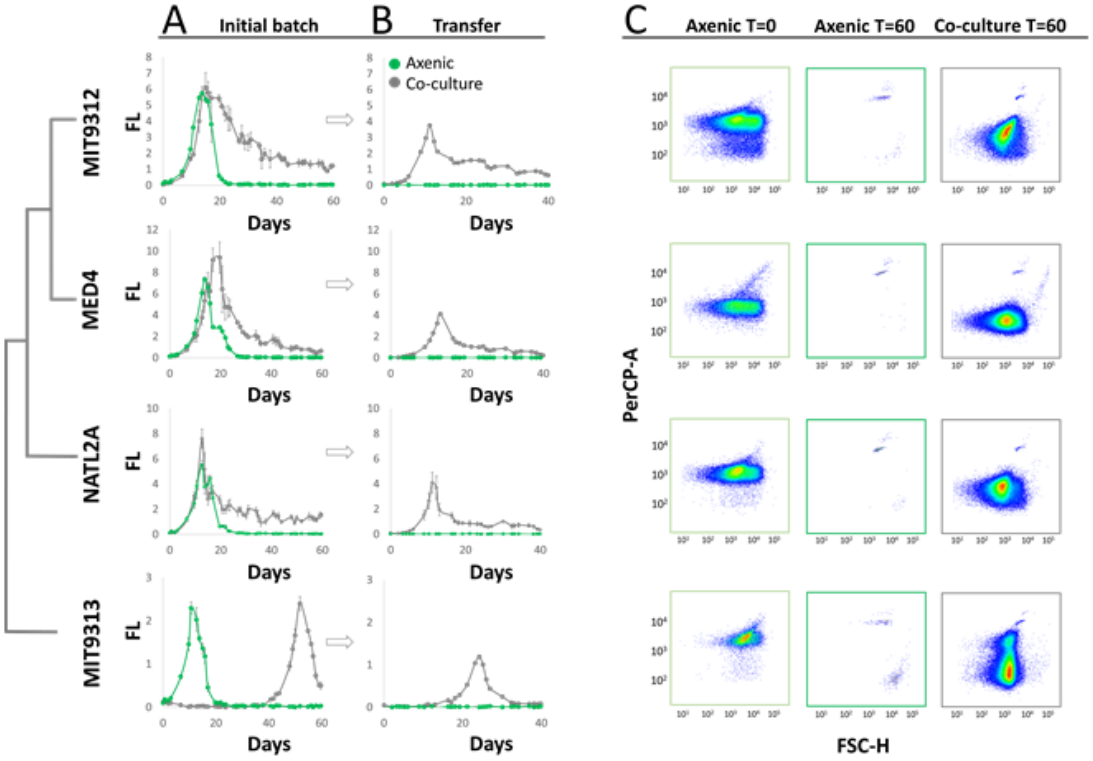
A
Initial batch
B
Transfer
C
Axenic T=0
Axenic T=60
Co-culture T=60
Axenic
Co-culture
MIT9312
MED4
NATL2A
MIT9313
FL
Days
PerCP-A
FSC-H